Comparisons between Active Properties of Distal Dendritic Branches and Spines: Implications for Neuronal Computations

Gordon M. Shepherd and Thomas B. Woolf

Section of Neuroanatomy
Yale University School of Medicine

Nicholas T. Carnevale

Department of Neurology
SUNY Stony Brook

Abstract

The specific contributions of distal dendrites to the computational properties of cortical neurons are little understood and are completely ignored in most network simulations of higher brain functions. Compartmental models, based on realistic estimates of morphology and physiology, provide a means for exploring these contributions. We have pursued analysis of a model of synaptic integration in a distal dendrite bearing four spines, using a new general-purpose simulation program called SABER. We have analyzed this model under the assumption that the dendrite contains sites of impulse-generating membrane, and we have compared its responses to synaptic activation with the case of impulse-generating membrane located instead in the spine heads, as previously reported. Both types of models generate basic logic operations, such as AND, OR, and AND-NOT gates. Active spine heads require lower excitatory synaptic conductances, but active branch segments lead to larger responses in the soma. The transients recorded near the soma give no evidence of their origin in either active branch or active spines, indicating that the interpretation of experimental recordings with regard to sites of distal active responses must be viewed with caution. The results suggest the hypothesis that a hierarchy of logic operations is virtually inherent in the branching structure of dendritic trees of cortical pyramidal neurons. Inclusion of these properties in representations of cortical neurons would greatly enhance the computational power of neural networks aimed at simulating higher brain functions.

Introduction

The functional significance of the distal dendrites of cortical pyramidal neurons is still unclear. Experimental studies are providing increasing evidence for a wide range of physiological properties. Among the most interesting from a functional point of view are voltage-gated membrane channels. Several different types of voltage-gated channels within dendritic trees have been identified which contribute to either rapid or slow impulse generation (Llinás 1988; Hounsgaard and Midtgaard 1989; McCormick 1989). Other types of synaptic channels with voltage-gated properties are believed to play a role in memory mechanisms (reviewed in Brown et al. 1988).

The remoteness of distal dendrites from recording sites at the soma has made analysis of these physiological properties difficult (see Figure 1a). Computational models have therefore been introduced to aid in exploration of these properties. These models were first used to analyze the spread of synaptic potentials in dendritic trees

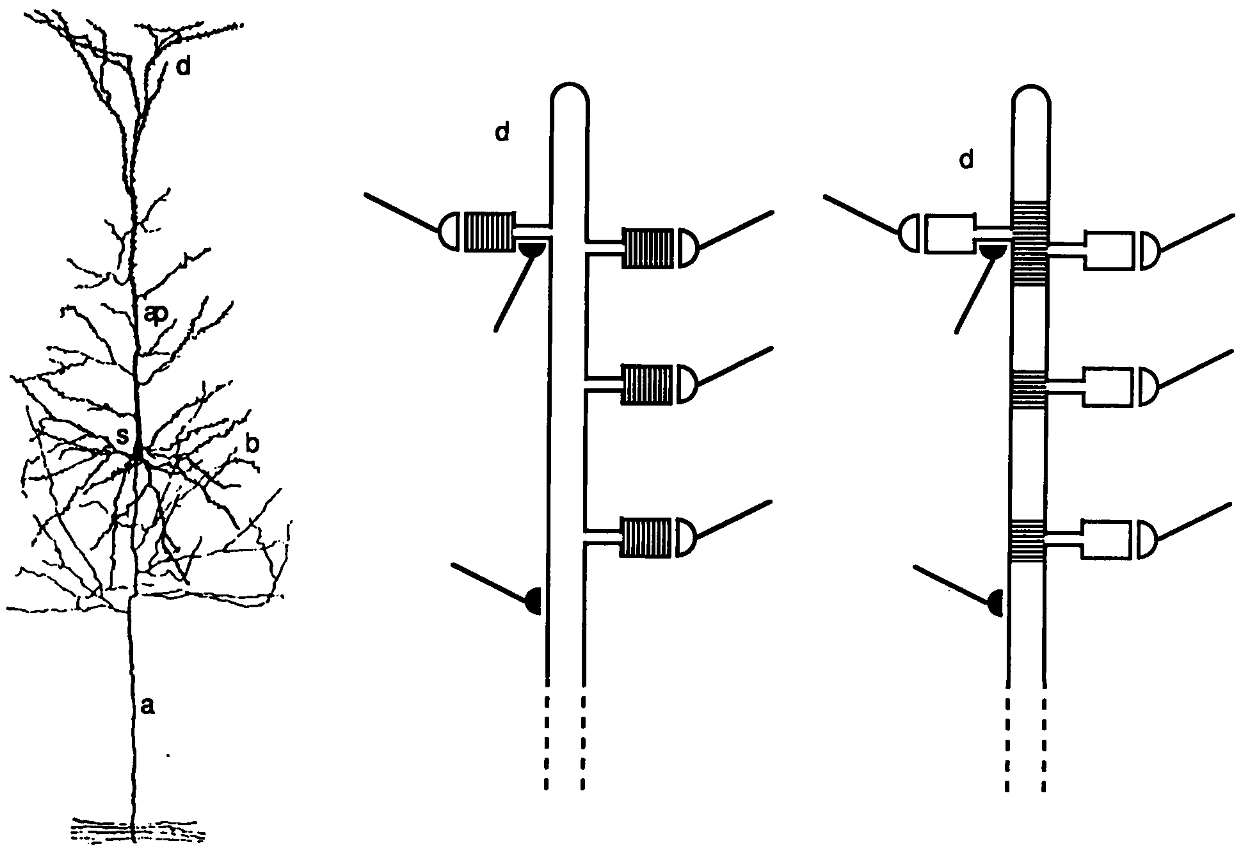

A. Cortical pyramidal neuron

B. Active spines, passive dendrite

C. Passive spines, active dendrite

Figure 1. Model for exploring the computational properties of spiny dendrites of cortical pyramidal neurons. (A) Golgi-stained cortical pyramidal neuron, after Cajal (1911). Abbreviations: *s*, soma; *ap*, apical dendritic trunk; *d*, distal dendritic branches; *b*, basal dendrites; *a*, axon. (B) Schematic representation of distal dendritic branch (D), bearing four spines, each of which contains active impulse-generating membrane. Each spine receives an excitatory synapse (open profiles) which may or may not be activated. Inhibitory synapses, which also may or may not be activated, to the spine neck or dendritic branch are shown as filled profiles. This model was explored by Shepherd and Brayton (1987). (D) Same model, but with the active membrane located instead in the dendritic branch at the base of the spines. This model is explored in this paper.

with passive membrane properties (Rall 1964). They were expanded to include voltage-gated properties (Rall and Shepherd 1968), and since have been used to simulate experimental findings regarding synaptic integration and impulse generation in a variety of neurons (see Dodge and Cooley 1973; Traub 1977; Pellionisz and Llinás 1977; Traub and Llinás 1979; Koch et al. 1982; Miller et al. 1985; Perkel and Perkel 1985; Shepherd et al. 1985). The use for this purpose of general circuit analysis programs (Shepherd and Brayton 1979; Bunow et al. 1985) has greatly facilitated this work, enabling the experimenter to simulate with relative ease any type of membrane property in any arbitrary distribution throughout a dendritic tree.

The problem we address in this study arose out of recent work indicating that the presence of active conductances in spines would confer interesting computational properties on distal dendrites and enhance their ability to communicate with the soma (cf. Miller et al. 1985; Perkel and Perkel 1985; Shepherd et al. 1985; Rall and Segev 1987; Shepherd and Brayton 1987; Segev and Rall 1988). In the course of this work we found that interactions between active spines can generate simple logic operations (Shepherd and Brayton 1987). In the present study, we wished to test whether these operations are limited to the case of active spines or whether they could arise, and arise as effectively, if the active channels are instead located in the dendritic branches (see Figure 1b, c). The results give insight into the ways that neurons may optimize their deployment of membrane channels to achieve specific functional capabilities. They also give further support to the idea that the computational power of distal dendrites is significant and should be incorporated into neural network models of higher cortical functions.

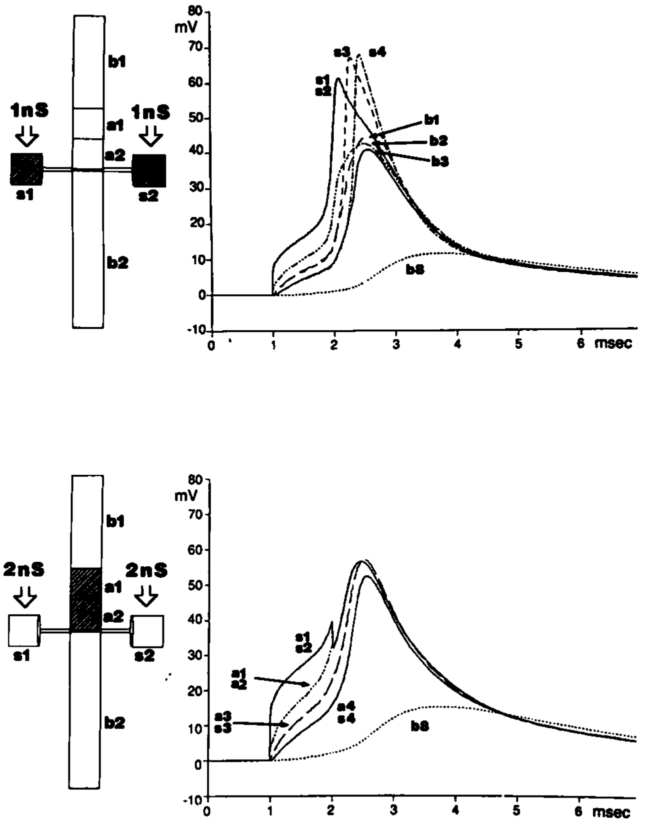

Figure 2. AND gate: Simultaneous synaptic excitation of spines 1 and 2, under assumptions of active membrane in the spine heads (upper diagram) and in the dendritic branch (lower diagrams). On the left are shown schematic diagrams of parts of the model, which include the two spines receiving the synaptic excitation (s1 and s2), and the neighboring branch segments (a1, a2; b1, b2). Upper diagram: excitatory synaptic conductances of 1 nS in spines s1 and s2. On the right, plots of the responses in the four spine heads of the model (s1–4), and four branch segments (b1–3 and b8; see full model in Figure 2 bottom). Synaptic conductance is turned on between 1 and 2 msec. These responses are similar to the responses in Shepherd and Brayton (1987). Lower diagram: Active membrane segments (a1–4) have same length (1 μm) and diameter (1 μm) as spine heads. Excitatory synaptic conductances of 2 nS are required to reach impulse threshold, as shown on the right. Note sharp onset and offset of EPSP in s1 and s2, due to step changes in synaptic conductance. This permits much more direct assessment of the effect of electrotonic properties on the response than is the case when the synaptic conductance is generated by a smooth function.

Results

As explained in *Methods*, the model consisted of a dendritic branch bearing four spines (see Figure 1c). Excitatory synaptic input could be delivered to spines 1 or 2 in the model. These spines thus represented a possible logic gate; spines 3 and 4 served to monitor the output of the gate.

Paired Excitatory Inputs (AND Gate)

We initially carried out a variety of simulations with active membrane in the spine heads, as a baseline to give assurance that the results using SABER were identical to those produced in the previous study of this model system by ASTAP (Shepherd and Brayton 1987). This is not a trivial point. One of the advantages of the reduced system of a single branch and only four spines is that the model is as constrained as possible; small changes in a response give direct insight into the specific details of the model which produced them.

With identical properties to those used previously, the model responded to simultaneous inputs to spines 1 and 2 with the complex responses shown in Figure 2 (top). The synaptic conductance was 1 nS in both spine 1 and 2, which was sufficient to reach threshold for activating the impulse (see peaks s1, s2). The impulses spread passively into the branch (b 1–3) and further into spines 3 and 4, where they were of sufficient amplitude to reach threshold for impulse activation (s3, s4). There was further spread by passive means through the branch to the proximal end compartment (b8) in the direction of the soma. Despite the complex nature of the nonlinear activity in the spines, the transients are virtually identical to those in our previous study using ASTAP (cf. Figure 2, Shepherd and Brayton 1987).

The basic question addressed in the present study is illustrated in Figure 2 (bottom). As indicated on the left, the active conductances were placed in the membrane of the dendritic branch rather than the spine heads. We started with the case in which the amount of conductance and the area of the membrane were exactly the same. In the example shown, the same amount of conductance in the two active spine heads was placed instead in two active branch segments (a1, a2) at the base of the spines. The branch segments also had the same dimensions (1-μm diameter and 1-μm length) as the spine heads. Thus, in terms of voltage-gated channels, the branch compartments had conductances representing the same number of channels at the same density as in the experiments with active spine heads.

We then asked, "How much excitatory synaptic conductance in the spine heads is needed to bring the system to threshold for spike generation?" The simulation showed that, keeping all other parameters constant, the 1-nS synaptic conductance was no longer adequate. In order to reach threshold, approximately 2 nS was required, as indicated in Figure 2 (bottom). There was,

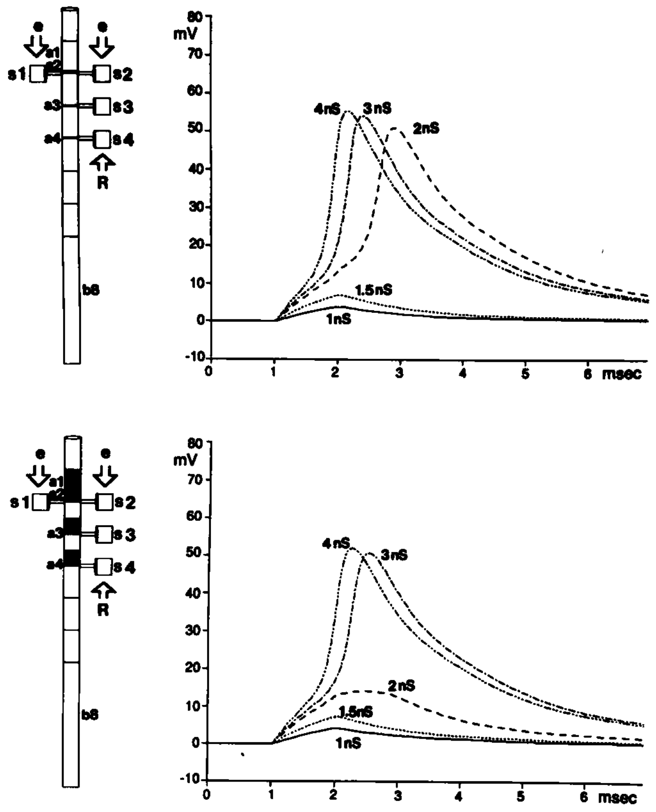

Figure 3. Effect of different extents of active branch membrane on the AND gate. Upper diagram: simultaneous synaptic excitation to spines 1 and 2, as in Figure 2. Complete model is shown, with active membrane segments of 1-μm length at the base of each spine (a1–4). On the right: graph of responses recorded in spine 4 for different values of the synaptic conductances in spines 1 and 2. Lower diagram: active membrane segments containing same total active conductances for Na and K in the H-H model have been increased to 25 μm in length (diameters are still 1 μm). On the right: recordings of responses in spine 4 show failure of 2 nS synaptic conductance to generate impulse response.

therefore, a raised threshold for synaptic activation of the active membrane in this configuration. The responses showed some additional features of interest. Since there was no active membrane in spines s1 and s2, the potentials in these compartments are limited to the excitatory postsynaptic potential (EPSP) generated there, to which is added the passive spread of the onset of the impulse activity generated in the active branch compartments (a1, a2). The overlap of the traces allows one to determine precisely the contribution of each of these components to the response.

The impulse activity generated in active branch compartments a1 and a2 spread to similar active compartments (a3, a4) situated at the bases of spines 3 and 4, respectively. Because of the short electrotonic distances for passive spread along the branch between these compartments, impulse activation was nearly simultaneous (Figure 2, bottom), compared with the clear sequence of activation when the active membrane was in the spine heads (Figure 2, top). Despite this, the impulse peaks reached only 54–58 mV, compared with 62–69 mV for the active spines. The impulse peaks in the branch and the spines are virtually identical (see a3, s3, and a3, s4 in Figure 2 bottom). This is because there is almost no electrotonic decrement when the impulse spreads from the branch into a spine, due to the short length of the spine neck and the boundary condition associated with the spine head. This is in marked contrast to the case of active spines, in which there are large differences between the peaks of activity in the spines (s1–s4) and branches (b1–b3) (see Figure 2 top), due to the impedance mismatch between spine and branch for activity spreading from spine to branch.

A final difference between the two cases is the response recorded in the most proximal branch compartment (b8), which is larger (15 mV) than for the case of active spines (12 mV) (see Figure 2). This is due largely to the impedance mismatch faced by the active spines, so that the impulses spreading passively into the branch compartments (b1–b3, top) have lower peaks (41–45 mV) than the impulses generated by the active branch compartments (54–58 mV for peaks in Figure 2 (bottom). We will return to this point below.

Sensitivity to Synaptic Conductance

In determining the level of synaptic conductance for achieving spike threshold, we explored the effect of different magnitudes of synaptic conductance on the responses. Typical results are shown in Figure 3, which includes on the left diagrams of the full compartmental model. In the top diagram, the same model is shown as in the bottom of Figure 2, with different synaptic conductances at (e) while recording from spine 4 (R). As can be seen, there was a rather sharp threshold; 1 nS and 1.5 nS (values for each of the two synapses) gave only passive responses, whereas 2 nS gave a full-blown impulse, as noted above. With increased synaptic conductance (3 nS, 4 nS), the latency decreased and the peak amplitude increased from 54 mV to 58 mV. It is obvious, therefore, that although the spike is an all-or-nothing event, the spike latency and spike amplitude are quite sensitive to the EPSP amplitude.

Sensitivity to Active Membrane Distribution

We next inquired into the effect on impulse threshold of changes in the distribution of the active membrane in the dendritic branch. We held the amounts of the voltage-gated conductances constant, but distributed them over increasing extents of branch membrane by increasing the lengths of the four active branch segments. Starting with the length of 1 μm used in Figure 2 (bottom) and Figure 3 (top), we investigated lengths of 2, 5, 10, 25, and 50 μm. The general finding was that as the length in-

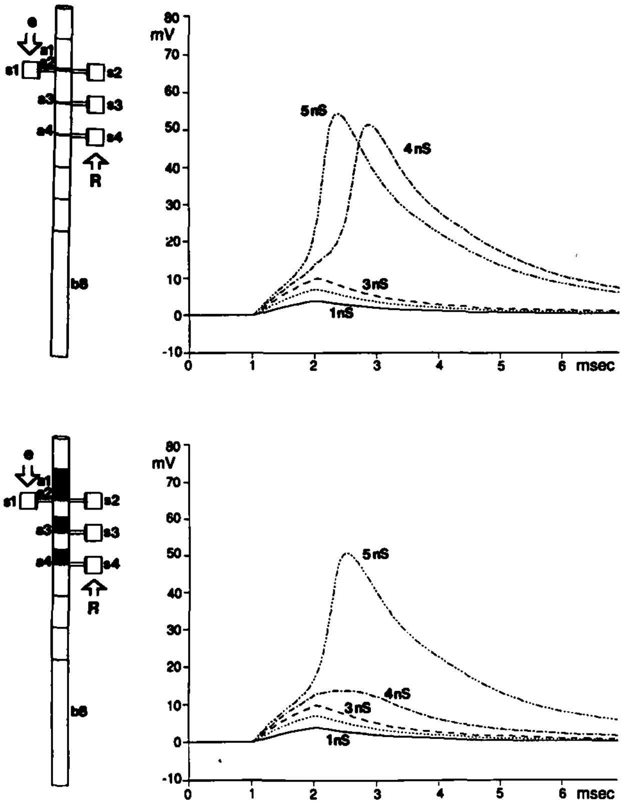

Figure 4. OR gate: Effects of different extents of active branch membrane on the response when synaptic excitation is delivered to only one spine. Same protocol as in Figure 3. Upper diagram: graph on right shows successful impulse generation with 4-nS synaptic conductance in spine 1 and active Na and K channels in 1-μm length branch segments. Lower diagram: active membrane segments containing same total active Na and K conductances of the H-H model have been increased to 25 μm in length. Graph on right: excitatory synaptic conductance of 5 nS required to reach impulse threshold.

creased, the impulse threshold rose. At 10 μm, the impulse response to 2 nS excitatory synaptic conductance was much delayed. At 25 μm (see Figure 3, bottom), 2 nS gave instead a low-amplitude, prolonged response indicating partial subthreshold activation of the voltage-gated Na conductance in the impulse model. Impulse threshold was reached by a synaptic conductance of 3 nS. This impulse has a slightly shorter latency than the threshold impulse generated by the 1-μm active segments, but a slightly lower amplitude (cf. top and bottom in Figure 3).

Effects of Changes in R_m

The effects of different assumptions for the value of the specific membrane resistance (R_m) were generally predictable. For the model illustrated in Figure 2, decreasing R_m from 4,000 to 1,000 ohm cm^2 raised the synaptic conductance required to reach impulse threshold from 2 nS to 3 nS and lowered the peak amplitude of the impulse. These effects were a direct consequence of the increased membrane conductance. It is interesting that these effects were very similar to those produced by spreading the active channels over large lengths of branch segments (Figure 3). With lower R_ms, the EPSP became too small to reach impulse thresholds. Higher R_ms were associated with larger EPSPs, briefer impulse latencies, and large impulse amplitude. Repolarization following the impulse was also delayed; with an R_m of 10,000 ohm cm^2, there was only partial repolarization, leading to a second abortive impulse. This was due to a combination of the longer membrane time constant which slowed the repolarization process, the much shorter electrotonic length of the branch which increased the effect of the boundary conditions in reflecting back the membrane potential changes, and partial Na inactivation in the H-H model. Miller et al. (1985) have explored similar properties of compartmental models which simulate epileptiform burst firing in distal dendrites. The present results thus reconfirm the evidence from computational studies that, because of their high input resistances, thin distal dendrites require only a modest value of R_m and relatively few ionic conductance channels to generate large and rapid changes in their membrane potential.

In addition to the effects of R_m, we have explored related factors bearing on impulse generation. Larger branch diameters were associated with lower input resistances, and lower adjustments of kinetic parameters and of the peak conductances of the H-H model were associated with slower action potentials with higher thresholds. The range of R_m producing the changes noted above is therefore dependent on many factors, all of which require further refinement with experimental data. These considerations also apply to the other types of logic gates described below.

Single Synaptic Inputs (OR Gate)

A single synaptic input directed to either spine 1 or spine 2 could lead to impulse generation in the active branch model, but it required an increased synaptic conductance. As shown in Figure 4 top, a single active synapse on a spine required a conductance of 4 nS in order that the EPSP have sufficient amplitude to reach spike threshold. It has previously been shown that, for the case of active spines, the amount of single synaptic conductance needs to be doubled approximately in order to be equivalent to the paired synaptic inputs in eliciting impulses (Shepherd and Brayton 1987). A similar rule appeared to apply to the case of an active branch. Thus, the 4-nS transient in Figure 4 (top) is identical to the threshold transient generated by two 2-nS synaptic conductances in the otherwise identical model of Figure 2 (top).

The sensitivity to different synaptic conductances also gave similar results. As shown in Figure 4 (top), the subthreshold and suprathreshold responses to a single synapse were generally equivalent to the responses generated by two synapses each of which had half the conductance, as in Figure 3. The effect of distributing the active membrane over greater lengths of the branch followed a similar rule, as can be seen in the subthreshold and suprathreshold responses of Figure 4 (bottom).

Paired Excitatory and Inhibitory Inputs (AND-NOT Gate)

One of the most important operations carried out by cortical neurons is the integration of excitatory and inhibitory synaptic inputs. If the inhibitory synapse is placed in such a way as to gate in a specific manner the communication of an excitatory synapse with the rest of a dendrite, the interaction can be regarded as an AND-NOT gate (Koch et al. 1982; Shepherd and Brayton 1987).

As in our previous study, we have investigated two configurations of this type of interaction. In the first, an inhibitory synapse directly gates a single spine by being placed on the spine head, spine neck, or at the base of the spine neck. These are common sites for placement of an inhibitory synapse (see Freund et al. 1984; Harris and Stevens 1988). This model is shown on the left in Figure 5 (top). We focus on the case in which the active membrane was confined to 1-μm length segments of the dendritic branch. An excitatory synaptic conductance of 4 nS for a single input to spine 1 was used; by itself, this was sufficient to reach impulse threshold, as shown previously in Figure 4 (top). This impulse response was little affected by a concurrent very weak inhibitory conductance of only 0.1 nS, as shown in Figure 5 (top). Note in this graph the very large EPSP in spine 1 (s1), where it is generated; the decrement of the EPSP in spreading passively into the branch (a1, a2); the beginnings of an active response in the branch, producing a rising transient before being terminated by turning off the synaptic conductance; and the continued activation of the voltage-gated Na conductances to give rise to a delayed impulse. The transients in spines 2–4 follow the transients in the branch segments a2–4 so closely that they are indicated as being identical; as mentioned above, this is because there is practically no decrement of potential in spreading passively from the branch into a spine. The impulse in spine 4 (s4) is similar to that in Figure 4 (top) (4 nS).

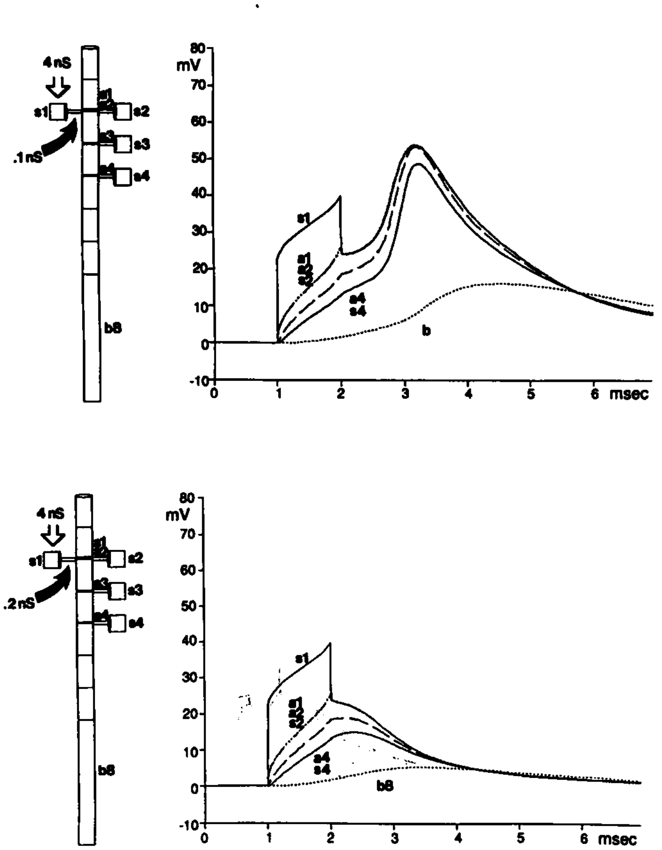

Figure 5. AND-NOT gate: Synaptic excitation (4 nS) is delivered to spine 1 while synaptic inhibition of 0.1 nS (upper diagram) and 0.2 nS (lower diagram) is delivered to the neck of spine 1. Active membrane is localized to 1-μm length segments of the dendritic branch. On the right: recordings of responses generated in spines 1, 2, and 4, active segments a1, a2, and a4, and proximal passive dendritic compartment b8.

Although this small amount of inhibitory conductance thus had little effect on the excitatory response, a slight increase to 0.2 nS resulted in complete suppression. Close analysis showed that the active response started to rise slowly during the synaptic conductance change, as before, but it was reduced by about 1 mV, which was sufficient to cause the active branch membranes to give only a subthreshold response before returning to baseline. The fact that only a 100-pS difference in inhibitory conductance produces this dramatic effect indicates that this configuration is very sensitive to inhibitory gating of the excitatory response. This is in contrast to the case of active membrane in the spine head, which requires a much stronger inhibitory conductance change (2 nS in the comparable model; see Shepherd and Brayton 1987, Figure 8) to block the excitatory response.

A contrasting configuration for excitatory-inhibitory interactions occurs when the inhibitory synapse is placed on a proximal segment of the branch, at a distance from the activated spine. This is depicted in Figure 6, which shows the inhibitory input on segment b7. In the previous study, it was found that the four active spines generated so much active current that it overwhelmed an inhibitory synapse at this location, so the model was reduced to three spines and the IPSP given an equilibrium potential increased from −5 mV relative to rest to −20 mV (Shepherd and Brayton 1987). When this model was adapted for active branches, it was found that an excitatory synaptic conductance of 6 nS sufficed to generate an action potential in the branches (Figure 6 top). An inhibitory conductance of 6 nS was not sufficient to affect this impulse, but an increase to 7 nS caused suppression (Figure 6 bottom). The slight initial hyperpolarization of the neighboring segment b8 is due to the hyperpolarizing equilibrium potential for this inhibitory conductance

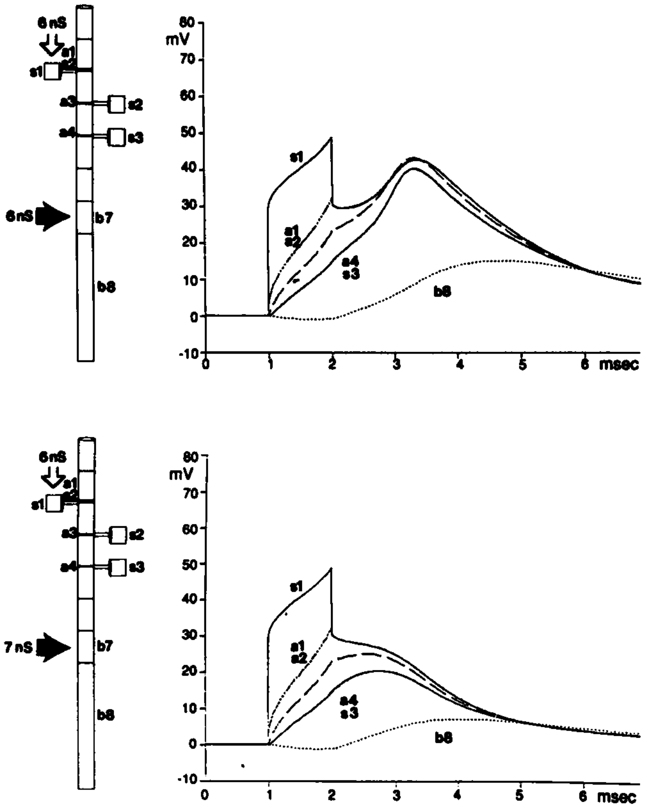

Figure 6. AND-NOT gate: Synaptic excitation (6 nS) is delivered to spine 1 while synaptic inhibition is delivered to a proximal dendritic compartment b7. Model is reduced to three spines; also, equilibrium potential of inhibitory conductance is increased from −5 mV relative to rest to −20 mV, to conform with model of Figure 9 in Shepherd and Brayton (1987).

(see b8 in Figure 6). This result contrasts with that of active spines, because although the same placement of inhibition could suppress downstream impulses, it could not affect generation of the initial impulse within the first spine (Shepherd and Brayton 1987).

Fast Prepotentials

Active dendritic properties are believed to be responsible for fast prepotentials when recorded at the soma, and it was therefore of interest to analyze the nature of the transients that would be recorded at or near the soma. An approximation is provided by the responses recorded in the proximal dendritic branch segment (s8), several hundred microns from the most proximal spine. We were particularly interested in how the transients generated by the active branch segments compare with those generated by active spines from this vantage point near the soma.

As typical examples, the transients in b8 from the experiment of Figure 2 are plotted together in Figure 7. As already noted, the peak of the active branch transient is about 25% greater than the peak of the active spine transient. It should be emphasized that in both cases the only active membrane is in the more distal compartments; the b8 transient is due to passive spread, controlled by the electrotonic properties of the system. The effect of these properties is to smooth the envelope of the transients generated in the more distally located active compartments, so that the proximally recorded summed transient has a smooth time course; there is no evidence of the sharp peaks and differences in timing of the individual action potentials in either the active spines or the active branches, or of the individual EPSPs generated in the passive spines (cf. Figure 2). This summed transient may appear as a slow potential on a relatively fast time base, in which case it would resemble an EPSP generated nearer to the soma. Alternatively, it may appear as a fast potential on a relatively slow time base (inset in Figure 7), in which case it would resemble the classically recorded fast prepotential due to impulse generation at a distant site.

Discussion

The main result of the present investigation is that voltage-gated conductances in a dendritic branch can provide the means for specific integration of synaptic inputs to spines in a manner that simulates simple logic operations. The use of logic operations as a paradigm enables us to make detailed comparisons of this result with other distributions of active membrane. We will summarize the comparison with active membrane in spines and then discuss the implications for neuronal function.

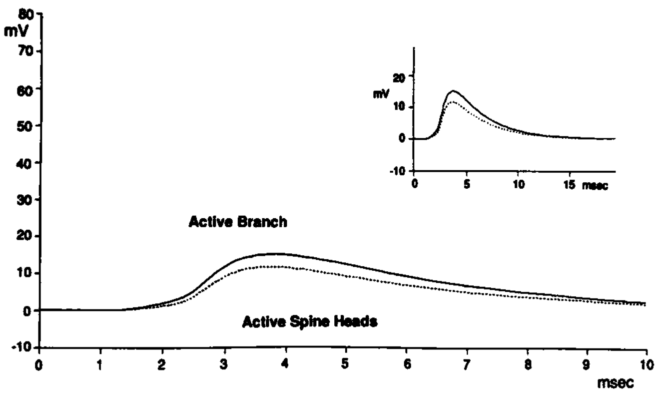

Figure 7. Comparison between the transients recorded in proximal dendritic compartment b8, for the case of active dendritic branch segments and active spine heads. Transients are from the analysis of the AND gate, illustrated in Figure 2. The inset shows the same transients on a slower time sweep. See text.

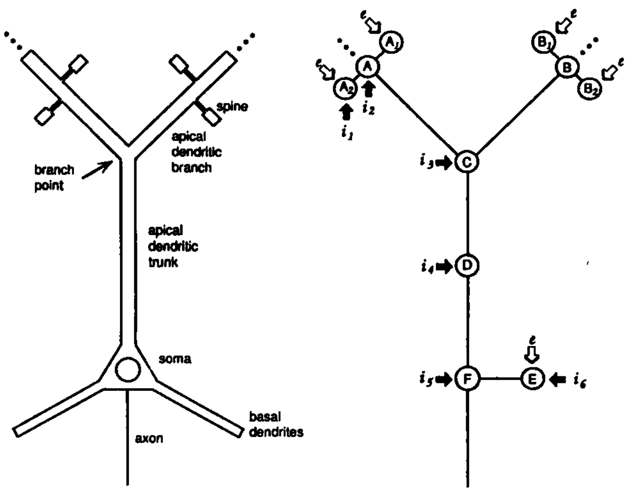

A. Schematic representation of reduced pyramidal neuron

B. Pyramidal neuron as a branching system of nodes for logic operations

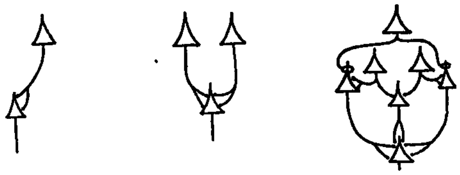

C. Original McCulloch-Pitts representation of neurons as oversimplified nodes for logic operations

Figure 8. The "canonical pyramidal neuron" as a substrate for a hierarchy of logic operations. (A) Schematic representation of the minimum architecture needed to capture the essential integrative structure of a cortical pyramidal neuron. (B) Compartmental representation of the canonical pyramidal neuron as a branching system of nodes for carrying out a hierarchy of logic operations. The operations explored in this paper and in Shepherd and Brayton (1987) at the synaptic, spine, and branch level are indicated by A, A1, A2 and B, B1, B2. Summing between these branches occurs at (C); gating of their linkage to the soma occurs in the apical trunk at (d); separate basal dendritic compartments are shown at (E); global dendritic and somatic summation takes place at the soma, (F). Inhibitory synaptic inputs (i1–i6) provide for possibility of AND-NOT operations at all levels of the logical hierarchy. (C) For comparison, these diagrams illustrate the McCulloch-Pitts representations of cortical neurons as simple nodes for the purpose of simulating circuits for logic operations (McCulloch and Pitts 1943). Note that the dendrites are totally ignored in these models.

AND Gate

The simulations show that active membrane in a branch can generate an impulse in response to simultaneous EPSPs in two nearby spines. We find that the most effective placement of the active membrane is in a small area. As the same amounts of voltage-gated conductances (same number of channels) are spread over larger areas of the branch, the amount of synaptic conductance necessary to reach impulse threshold increases. The effect is relatively modest; in going from a length of active membrane segment of 1 μm to 50 μm, the threshold increase is approximately twofold. Thus, the least effective placement of voltage-gated channels is an even distribution at low density over the entire branch; the most effective is a high density of channels in a small area. This is reminiscent of the clustering of active channels at nodes of Ranvier, for efficient saltatory impulse conduction in myelinated axons.

Even in their most effective distribution, the voltage-gated channels in the branch were less effective than in the spine heads, where the EPSPs are generated. This supports the prediction of Rall and Segev (1987) that the lowest threshold for synaptic activation of dendritic impulses is associated with placement of the voltage-gated channels in spine heads. The fact that our model assumed slightly faster H-H kinetics and somewhat lower spine input resistances (see *Methods*) supports the generality of this proposition (see also Perkel and Perkel 1985; Miller et al. 1985; Shepherd et al. 1985). Under the conditions of our model, the spine heads were more effective compared with branch segments equal in membrane areas and amounts of voltage-gated conductances (i.e., equal densities and numbers of conductance channels) by a factor of approximately 2. These results might suggest, therefore, that this is the most effective placement for generating the AND operation.

The simulations, however, reveal other factors that need to be taken into account in assessing what is meant by "most effective." One is the fact that the impulse spreading in the branch is larger in amplitude (by about 25% in the present simulations) when the active membrane is in the branch than when it is in the spine heads. This can be viewed as counterbalancing the higher synaptic conductance that is required by the active branch configuration, in effect moving the site of generation closer to the cell body to control impulse output in the axon hillock. A second point is that the impulse peaks in spine heads are higher when the impulses are generated there than when they are generated in the branch segments. Coupled with this is a large disparity between peak depolarizations in the spine heads and the branch, whereas when the branch is active, the spine head depolarizations follow the branch depolarizations very closely (except for the initial EPSPs). This is of interest in view of recent evidence that the differential depolarization of synaptically activated spines may be functionally important, particularly for mechanisms underlying LTP (see Brown et al. 1988). A third point is that the pseudosaltatory conduction of the impulse is much faster between active branch segments than it is between active spines.

OR Gate

Most of the electrotonic factors involved in the AND gate also are relevant to the mechanism of the OR gate. As shown previously (Shepherd and Brayton 1987), there is a scaling rule that the same synaptic conductance placed in one spine or distributed between two spines will have an approximately equal depolarizing effect in the branch. This rule applies also in the present simulations, in which the synaptic conductance in a single spine required to reach impulse threshold was approximately twice that required in two spines. The rule is not exact; doubling the synaptic conductance in one spine does not double the EPSP, because of the loading effect of added conductance channels and the nearer approach to the equilibrium potential of the ions involved (Rall 1964). It was a reasonable approximation in the present case because of the relatively modest synaptic conductances and EPSP amplitudes required. The OR gate was less effective with wider distribution of the voltage-gated conductances in the branch. There were differences in the electrotonic properties of the spreading impulses from those of impulses generated in the spine heads, as discussed above.

It seems clear from these considerations that a dendritic branch might be changed between acting as an OR gate and an AND gate by relatively small shifts in its membrane properties. A useful distinction might therefore be made between fixed ("hard-wired") gates and reprogrammable ("soft-wired") gates. For example, an excitable branch with passive spines would function as an AND gate if coactivation of inputs to several spines is required to drive the branch past threshold. This AND would be "soft" or dynamically reprogrammable to an OR if the spine neck resistances are small so that an increase of synaptic conductance on one of the spines could elicit a spike by itself. Such an increase might result from developmental or use-dependent changes of transmitter release, receptor density, etc. On the other hand, large spine neck resistances could limit the current that any spine could contribute, regardless of the size of the synaptic conductance. Such an arrangement would constitute a relatively "hard" or fixed AND, although it could be modified by changes in spine neck properties.

It was previously noted that single active spines functioning as OR gates would be more likely in thin distal dendrites, where the higher input resistance would produce larger potentials for given amounts of conductance increases and associated ionic currents (Shepherd and Brayton 1987; see also Segev and Rall 1988). The same reasoning would apply to OR gates set up by active sites on branches. The tendency of any given input to fire the cell would be opposed by the large conductance load of the rest of the dendritic tree faced by any single response in one part of the tree, requiring coincident firing of more proximal branches in order to affect the soma (Rall and Segev 1987).

AND-NOT Gate

The simulations tested two basic relations between an inhibitory and an excitatory synapse: inhibition at the site of excitation and at a distance on the route to the soma. There are important functional differences between these two arrangements, and our results also demonstrate important differences between the cases of active spines and branches.

When inhibition was placed on the neck of a synaptically activated spine, it was extremely effective in blocking spread of the EPSP to generate an impulse in the branch. This result is in line with a variety of studies showing the effectiveness and selectivity of inhibition sited on a spine for opposing excitation in the same spine (see Rall 1964; Jack et al. 1975; Segev and Parnas 1983; Koch and Poggio 1983; Segev and Rall 1988). In our model, the synaptic excitatory and inhibitory conductances occurred simultaneously, which maximizes the inhibitory effect (cf. Segev and Parnas 1983; Koch and Poggio 1983; Segev and Rall 1988). The amount of inhibitory conductance for blockade was extremely low, both in absolute amount (200 pS) and in the small difference between blockade and no blockade (100 pS). This is an order of magnitude smaller than the amount of inhibitory conductance required to block the impulse response of an active spine (Shepherd and Brayton 1987). Thus, the separation of the EPSP in the spine head from the site of active membrane in the branch creates a link that is much more susceptible to gating by inhibition than the case in which the active membrane is in the spine head at the site of synaptic excitation. In fact, in the latter case, the inhibition is actually downstream (more proximal to the soma) from the EPSP, which is well known to be unfavorable for opposing excitation (Rall 1964; Koch et al. 1982).

When inhibition is located instead at a proximal site on the branch, a relatively large inhibitory conductance is needed to block impulses generated in the branch. This is similar to the findings with simulations of a branch with active spines, except that the inhibitory conductances required are approximately twice as great. This is because the inhibition must act by directly opposing the impulse as it is generated and propagated in the branch itself, rather than by quenching the EPSP at its site of generation in the spine or by gating the spread of impulses from spine to spine.

Despite the large difference in amounts of inhibitory conductances, both placements of inhibition have very similar effects, causing a complete blockade of all impulse activity. By contrast, when the active membrane is in the spines, distant inhibition can gate the spread of impulse activation to neighboring spines but is relatively ineffective in opposing impulse generation in the spine receiving the excitatory input (Figure 9; Shepherd and Brayton 1987). Thus, there appear to be more varieties of inhibitory gating possible with active spines than with active branches, at least within this particular model system.

Interpreting Somatic Recordings of Dendritic Potentials

In electrophysiological experiments, activity in dendrites is customarily judged by recordings at the soma, and the simulations provide some useful leads to the interpretation of these recordings. Earlier studies identified rapid, low-amplitude spikes preceding large somatic action potentials in orthodromic responses to synaptic inputs. It was suggested that these "fast prepotentials" represent action potentials generated at "hot spots" in the dendrites, most likely at dendritic branch points. It was supposed that these prepotentials are small because they spread passively from their site of generation to the soma. The impulses were believed to boost the amplitude of dendritic synaptic responses in their effect on the soma (Eccles et al. 1958; Spencer and Kandel 1961; Llinás and Nicholson 1971). In a few instances, it has been possible to obtain more direct evidence for dendritic action potentials (Llinás and Sugimori 1980), confirming their large size in the dendrites and small size at the soma.

Our simulations support the idea of restricted active sites in the dendrites, with passive spread and its associated decrement to the soma. Most experimental evidence points to Ca conductance underlying active responses in dendrites rather than the traditional Na conductance of the H-H model, as used here. There are several varieties of Ca conductance (see Llinás 1988), each of which can be incorporated into the present model with suitable assumptions.

Considering the proximal dendritic segment as an approximation of the soma, we may ask whether the simulations shed light on whether dendritic action potentials are more likely to arise in active spines or active branches. The surprising answer is that, except for a slightly smaller amplitude, the soma transient generated by active spines is virtually identical to that generated by an active branch. Due to electrotonic smoothing, there is no evidence of the individual impulses generated in the periphery. The clear implication of this result is that there is no a priori reason to assume that a dendritic spike, recorded at the soma, is generated in a dendritic branch rather than in dendritic spines. Further experimental analysis is therefore required to distinguish between these two possibilities in any particular neuron. Given the range of methods that are becoming available, these tests should soon be possible; they might include patch recordings from dendrites, observations using ion-sensitive or voltage-sensitive dyes, or in situ hybridization for channel messenger RNA.

A further point relevant to the interpretation of electrophysiological recordings is that slower transients generated by active dendritic properties can overlap with the time course of synaptic potentials. Since each active site might make a very small contribution to the overall PSP recorded at the soma, it would be difficult to distinguish it from the contributions of individual PSPs. If the active conductances were in the dendritic spines, they could complicate the attempt to identify the conductance changes associated with the generation of the PSPs. There is not a clear terminology for these combined synaptic and active transients; are they actively enhanced EPSPs, or synaptically elicited action potentials? (See also Segev and Rall 1988 on this question.) These considerations suggest that distinguishing between the contributions of voltage- and ligand-gated conductances to the generation of composite potentials will not be an easy task. It will be useful to correlate experimental analysis with computational simulations in pursuing this important problem, as was done for the motoneuron (cf. Rall et al. 1967).

Implications for Neural Nets

The present results, taken together with previous reports (Rall 1970; Koch et al. 1982; Shepherd and Brayton 1987), justify the hypothesis that basic logic operations are virtually inherent in the structural and functional organization of neuronal dendrites, particularly those bearing spines. Unfortunately, a theoretical framework for assessing the contributions that these operations can make to multineuronal circuits and systems does not exist, first because dendrites have been traditionally completely ignored in the construction of neural nets to represent neural systems (McCulloch and Pitts 1943), and second, because current networks emphasize graded rather than thresholding operations (reviewed in Rumelhart and McClelland 1986). It will be useful therefore to indicate in a preliminary way how the present results may be incorporated into more realistic network architectures.

Incorporating Dendritic Functions into Network Nodes: Since dendritic trees are complex, and are distinctive for different neuronal types, it is desirable to reduce their complexity to a simpler level that still retains the essence of their functions. Based on the present simulations, the simplest model that captures the logic operations of the spiny dendritic tree of a cortical pyramidal cell is represented in Figure 8a. This shows a pyramidal neuron with an apical dendrite that gives rise to two branches, each of which gives rise to two spines. Figure 8b shows a simple compartmental model of this system, consisting of a soma (F), apical dendrite (D), two branches (A and B), and their spines (A1, A2 and B1, B2). Synaptic excitation (e) can be delivered singly or paired to each pair of spines; synaptic inhibition (i) can be delivered at any level of the system. One branch with its spines (e.g., A, A1, A2) is necessary in the model to generate the basic logic operations represented in this and the previous study; the other branch with its spines (e.g., B, B1, B2) is necessary to represent the fact that activity in any one part of a dendritic tree has to be integrated with activity in the other parts of the tree. Thus, the compartments A, A1, A2 and B, B1, B2 can represent individual logic gates or they can represent the combined logic operations carried out by their entire branch (indicated by the dotted lines), as suggested by Shepherd and Brayton (1987); see below.

In this model, each set of peripheral compartments (A, A1, A2 or B, B1, B2) carries out the logic operations described in the present paper. As shown here, logic operations are inherent in the arrangement of these compartments; they arise whether active membranes are in the spine heads or the branch. This level of the model captures the microphysiology of the single synapse and the single spine, and thus accurately reflects the organizational level of the single synapse, as well as the combined operations of multiple synapses and spines.

The next level of dendritic branching that is basic to all dendritic trees is represented by branches A and B in Figure 8. The branch point C is the crucial link between the local activity in the peripheral compartments and the global summation taking place at the soma. The summation of excitation at the branch point and its inhibitory gating there expresses at a more global level of organization the same types of logic operations carried out in the local regions of the periphery. The long apical dendrite (D) which is so characteristic of cortical pyramidal neurons ensures that the local computations are carried out relatively independently of the soma. Among other things, this limits the interference of soma impulse activity with the integration of synaptic responses and local active responses that underlie the peripheral logic operations. It also enables the summed effect of all the peripheral activity to be gated by inhibition in its last linkage to the soma. At the soma, impulse firing is contingent on summation of all dendritic activity, gated by global inhibition.

It may be noted that in the network literature, nodes are sometimes represented as having a long "dendrite." This, however, is only a graphical convenience for representing multiple inputs summing at that node and does not capture the contingent operations that take place in real dendrites, such as we have explored here.

These considerations indicate that there is a natural hierarchy of functional operations within a dendritic tree. Within this hierarchy are properties of logic operations at successive levels of branch organization. We have previously suggested that "a single dendritic tree can compute a very complicated logic function, one that can be proved to include any threshold function" (Shepherd and Brayton 1987). This suggestion may now be extended to the whole neuron to include the hierarchy of threshold computations as activity flows from local synaptic sites to global somatic summation.

This model may be compared to previous attempts to represent the dendritic architecture of pyramidal neurons for the purpose of building more realistic cortical networks. The pyramidal neuron of Traub and Llinás (1979) included two basal dendrites and an apical dendrite with two branches. Traub et al. (1989) have constructed networks containing up to 10,000 of these units, interconnected by both excitatory and (through interneurons) inhibitory synapses. The network has been used to explore the generation and spread of epileptic seizure activity, but not, thus far, cognitive functions. Wilson and Bower (1989) have represented the apical dendrite of the pyramidal neuron in olfactory cortex by a chain of three compartments, each receiving a specific type of synaptic input. These models thus include some of the integrative capacities of the apical dendrite, but not the level of interactions between single spines. They could be easily extended to include that level in the manner indicated in Figure 8a, b.

We have previously suggested that the pyramidal neuron, with its apical and basal dendritic structure and its distribution of spines for receiving synaptic inputs, is one of a set of elements that form a basic circuit unique to cerebral cortex (Shepherd et al. 1979, 1988; Kriegstein and Connors 1986). This same idea is contained in the "canonical cortical circuit" of Douglas and Martin (in press). The model in Figure 8 can therefore be regarded as a canonical pyramidal neuron, representing a generic computational structure that is elaborated and adapted for a family of related functions in different types of cortex. The task then becomes to define the complex function that represents this hierarchy and use it to replace the simple summing node of traditional neural nets.

Incorporating Thresholding Operations into Network Nodes: The present results may be regarded as building on the concept of McCulloch and Pitts (i.e., that thresholding operations are important in neural function), but placing many of those operations within dendritic trees. Several of the types of operations envisaged by McCulloch and Pitts are illustrated in Figure 8c, taken from their original paper. Comparison with Figure 8b suggests that, because of the local interactions within the dendritic tree, the output of a pyramidal neuron represents a complex transformation of its synaptic inputs which could otherwise be achieved only by interactions between several simple neurons. Thus, many of the functional operations believed to take place through interactions between simple nodes in neural networks may be mappable onto branching dendritic trees. A parallel might be drawn to the difference in scale between the rudimentary operations performed by individual logic gates and the much greater computational power of an LSI microprocessor (cf. Mead and Conway 1980; Mead 1989).

Current neural nets not only follow McCulloch and Pitts in neglecting the role of dendrites, but many have also eliminated the property of impulse generation. In these nets, the output of a node is represented by a variable that is a graded, linear or nonlinear function of the weighted sum of its inputs (Hopfield 1984; Rumelhart and

McClelland 1986). It is being realized that, in order to assess the neural properties of these networks, much more needs to be known about the computational properties and "styles" of real neurons (Sejnowski 1986; Koch and Poggio 1987). The present study attempts to contribute to that goal. The results support the idea that thresholding operations in dendrites are critical elements in the computational styles of real neurons. These results in turn are based on the growing experimental evidence for nonlinear voltage-gated and synaptic membrane properties, as cited above. The present study may therefore be a step toward incorporating real neural architectures and real neural properties into neural networks in order to obtain a more accurate representation of the true computational operating modes of cortical circuits and systems.

Methods

The computational methods build on previous studies in which general circuit analysis programs were adapted for application to neuronal modeling (ASTAP: Shepherd and Brayton 1979; SPICE: Bunow et al. 1985). In the present study, we use a new general simulator program termed SABER (Analogy, Inc.) (Flach et al. 1987; Carnevale et al. 1988; Shepherd et al. 1988). Like the other programs, this greatly facilitates the simulation of both linear and nonlinear membrane properties in any arbitrary distribution throughout a branching dendritic tree. In this program, the Hodgkin-Huxley equations for the impulse can be directly written into files, and kinetic parameters changed individually for any given run, as in ASTAP, but unlike SPICE. SABER's other improvements lie in its effective use of hierarchical templates in building a model. Examples of templates developed for the present models are given in Carnevale et al. (1988 and in preparation).

The dendritic system analyzed in the present study is identical in its basic structure to that of a previous study (Shepherd and Brayton 1987). As indicated schematically in Figure 1b, c, this consists of a length of distal dendritic branch giving rise to four spines. The branch diameter is 1 μm; the spine heads are 1 μm in length and 1 μm in diameter. The spine necks were 1 μm in length and were varied from 0.05 – 0.2 μm in diameter to explore the effect on spine-branch coupling. The system was represented as a compartmental model in the usual way (see Figure 1b, c; Figures 2 and 3); the specific forms of the model are indicated diagramatically in each figure in the *Results*. The models were explored using a range of values for R_m, as detailed in the text. However, in order to facilitate comparison between the different models of this study as well as with the active spine models of Shepherd and Brayton (1987), the results illustrated in this paper were all obtained under the assumptions of a specific membrane resistance of 4,000 ohm cm^2 and a specific internal resistance (Ri) of 80 ohm cm^2.

It may be noted that this model differs slightly from other models of dendritic spines in terms of details but not in ranges of parameters; thus, in the model of Segev and Rall (1988) for exploring properties of single spines, the spine necks tended to be thinner, the spine input resistance higher, and the specific membrane resistance lower; none of these differences introduced any significant inconsistencies between the two studies.

Active membrane properties were simulated by the Hodgkin-Huxley model (Hodgkin and Huxley 1952). As noted above, the effects of changes of kinetic parameters could be easily explored within the hierarchical format of SABER. For ease of comparison with previous results, we have used the same parameters as in Shepherd and Brayton (1987), which in turn were based on a series of studies in several laboratories concerned with adapting the H-H equations to mammalian neurons (Dodge and Cooley 1973; Pellionisz and Llinás 1976; Traub 1977; Traub and Llinás 1979).

Activation of a synapse was simulated by step increases in a depolarizing (excitatory) or hyperpolarizing (inhibitory) membrane conductance, lasting 1 msec. The abrupt conductance changes greatly facilitated analysis of the timing of responses and of the effects of electrotonic parameters on the properties of the responses. The basic functional properties discussed in this paper were not dependent on this particular time course, as shown by trials utilizing conductances controlled by alpha-functions (cf. Jack et al. 1975). The synaptic conductances are given in siemens, abbreviated S: 1 S = 1 mho (old terminology) = 1 ohm^{-1}; 1 nS = 1 nanosiemen = 10^{-9} S = 10^9 ohm^{-1}; 1 pS = 1 picosiemen = 10^{-12} S = 10^{12} ohm^{-1}.

Acknowledgments
This work has been supported by the National Institute for Neurological Diseases and Stroke (NS-07609) and the Office of Naval Research (N00014-86-K-01455).

References

Brown, T.H., Chang, V.C., Ganong, A.H., Keenan, C.L., & Kelso, S.R. (1988). Biophysical properties of dendrites and spines that may control the induction and expression of long-term synaptic potentiation. In P.W. Landfield & S.A. Deadwyler, (Eds.), *Long-term Potentiation: From Biophysics to Behavior*. New York: Alan R. Liss, 201–264.

Bunow, B., Segev, I., & Fleshman, J. (1985). Modeling the electrical behavior of anatomically complex neurons using a network analysis program: excitable membrane. *Biological Cybernetics*, *53*, 4–56.

Cajal Santiago Ramon, Y. (1911). *Histologie du Système Nerveux de l'Homme et des Vertèbrès*. Paris: Maloine.

Carnevale, N.T., Woolf, T.B., & Shepherd, G.M. (1988). Neuron simulations with SABER. *Society for Neuroscience Abstracts*, *14*, 300.

Dodge, F.A. Jr. & Cooley, J.W. (1973). Action potential of the motoneuron. *IBM Journal Research Division*, *17*, 219–229.

Douglas, R. & Martin, K.R. (in press). Neocortex. In G.M. Shepherd, (Ed.), *The Synaptic Organization of the Brain*, third edition. New York: Oxford University Press.

Eccles, J.C., Libet, B., & Young, R.R. (1958). The behaviour of chromatolysed motoneurones studied by intracellular recording. *Journal of Physiology (London)*, *143*, 11–40.

Flach, K., Carnevale, N.T., & Sussman-Fort, S.E. (1987). Neuron simulations using SABER. *Society for Neuroscience Abstracts*, *17*, 159.

Freund, T.E., Powell, J.F., & Smith, A.D. (1984). Tyrosine hydroxylase-immunoreactive boutons in synaptic contact with identified striatonigral neurons with particular reference to dendritic spines. *Neuroscience*, *13*, 1189–1215.

Harris, K.M. & Stevens, J.K. (1988). Dendritic spines of rat cerebellar Purkinje cells: serial electron microscopy with reference to their biophysical characteristics. *Journal of Neuroscience*, *8(12)*, 4455–4469.

Hodgkin, A.L. & Huxley, A.F. (1952). A quantitive description of membrane current and its application to conduction and excitation in nerve. *Journal of Physiology (London)*, *117*, 500–544.

Hopfield, J.J. (1984). Neurons with graded response have collective computational properties like those of two-state neurons. *Proceedings of the National Academy of Science USA*, *81*, 3088–3092.

Hounsgaard, J. & Midtgaard, J. (1989). Synaptic control of excitability in turtle cerebellar Purkinje cells. *Journal of Physiology (London)*, *409*, 157–170.

Jack, J.J.B., Noble, D., & Tsien, R.W. (1975). *Electric Current Flow in Excitable Cells*. Oxford, U.K.: Oxford University Press.

Koch, C. & Poggio, T. (1983). A theoretical analysis of electrical properties of spines. *Proceedings of the Royal Society of London Series B*, *218*, 455–477.

Koch, C. & Poggio, T. (1987). Biophysics of computation: neurons, synapses, and membranes. In G.M. Edelman, W.E. Gall, & W.M. Cowan, (Eds.), *Synaptic Function*. New York: Wiley, 637–698.

Koch, C., Poggio, T., & Torre, V. (1982). Retinal ganglion cells: a functional interpretation of dendritic morphology. *Philosophical Transactions Royal Society of London Series B*, *298*, 277–264.

Kriegstein, A.R. & Connors, B.W. (1986). Cellular physiology of the turtle visual cortex: Synaptic properties and intrinsic circuitry. *Journal of Neuroscience*, *6*, 178–191.

Llinás, R. (1988). The intrinsic electrophysiological properties of mammalian neurons: insights into central nervous system function. *Science*, *242*, 1654–1664.

Llinás, R. & Nicholson, C. (1971). Electrophysiological properties of dendrites and somata in alligator Purkinje cells. *Journal of Neurophysiology*, *34*, 537–551.

Llinás, R. & Sugimori, M. (1980). Electrophysiological properties of in vitro Purkinje cell somata in mammalian cerebellar slices. *Journal of Physiology (London)*, *325*, 171–195.

McCormick, D.A. (in press). Membrane properties and neurotransmitter actions. In G.M. Shepherd, (Ed.), *The Synaptic Organization of the Brain*, third edition. New York: Oxford University Press.

McCulloch, W.S. & Pitts, W.H. (1943). A logical calculus of the ideas immanent in nervous activity. *Bulletin of Mathematical Biophysics*, *5*, 115–133.

Mead, C. (1989). *Analog VLSI and Neural Systems*. Reading, MA: Addison-Wesley.

Mead, C. & Conway, L. (1980). *Introduction to VLSI Systems*. Reading, MA: Addison-Wesley.

Miller, J.P., Rall, W., & Rinzel, J. (1985). Synaptic amplification by active membrane in dendritic spines. *Brain Research*, *325*, 325–330.

Pellionisz, A. & Llinás, R. (1977). A computer model of cerebellar Purkinje cells. *Neuroscience*, *2*, 37–48.

Perkel, D.H. & Perkel, D.J. (1985). Dendritic spines: role of active membrane in modulating synaptic efficacy. *Brain Research*, *325*, 331–335.

Rall, W. (1964). Theoretical significance of dendritic trees for neuronal input-output relations. In R.F. Reiss, (Ed.), *Neural Theory and Modeling*. Stanford: Stanford University Press, 73–97.

Rall, W. & Segev, I. (1987). Functional possibilities for synapses on dendrites and on dendritic spines. In G.M. Edelman, W.F. Gall, & W.M. Cowan, (Eds.), *Synaptic Function*. New York: Wiley, 605–636.

Rall, W. & Shepherd, G.M. (1968). Theoretical reconstruction of field potentials and dendrodendritic synaptic interactions in olfactory bulb. *Journal of Neurophysiology*, *31*, 884–915.

Rumelhart, D.E. & McClelland, J.L. (Eds.) (1986). *Parallel Distributed Processing*. Cambridge, MA: The MIT Press.

Segev, I. & Parnas, I. (1983). Synaptic integration mechanisms: A theoretical and experimental investigation of temporal postsynaptic interactions between excitatory and inhibitory inputs. *Biophysical Journal*, *41*, 41–50.

Segev, I. & Rall, W. (1988). Computational study of an excitable dendritic spine. *Journal of Neurophysiology*, *60*, 499–523.

Sejnowski, T.J. (1986). Open questions about computation in cerebral cortex. In D.E. Rumelhart & J.L. McClelland, (Eds.), *Parallel Distributed Processing*. Cambridge, MA: The MIT Press, 372–389.

Shepherd, G.M. & Brayton, R.K. (1979). Computer simulation of a dendrodendritic synaptic circuit for self and lateral inhibition in the olfactory bulb. *Brain Research*, *175*, 377–382.

Shepherd, G.M. & Brayton, R.K. (1987). Logic operations are properties of computer-simulated interactions between excitable dendritic spines. *Neuroscience*, *21*, 151–166.

Shepherd, G.M., Brayton, R.K., Miller, J.P., Segev, I., Rinzel, J., & Rall, W. (1985). Signal enhancement in distal cortical dendrites by means of interactions between active dendritic spines. *Proceedings of the National Academy of Science USA*, *82*, 2192–2195.

Shepherd, G.M., Carnevale, N.T., & Woolf, T.B. (1988). Comparisons between computational operations generated by active responses in dendritic branches and spines. *Society for Neuroscience Abstracts*, *14*, 620.

Spencer, W.A. & Kandel, E.R. (1961). Electrophysiology of hippocampal neurons. IV. Fast prepotentials. *Journal of Neurophysiology*, *24*, 272–285.

Traub, R.D. (1977). Motoneurons of different geometry and the size principle. *Biological Cybernetics*, *25*, 163–176.

Traub, R.D. & Llinás, R. (1979). Hippocampal pyramidal cells: significance of dendritic ionic conductances for neuronal function and epileptogenesis. *Journal of Neurophysiology*, *42*, 476–496.

Traub, R.D., Miles, R., & Wong, R.K.S. (1989). Model of the origin of rhythmic population oscillations in the hippocampal slice. *Science*, *243*, 1319–1325.

Wilson, M.A. & Bower, J.M. (1989). The simulation of large-scale neural networks. In C. Koch & I. Segev, (Eds.), *Methods in Neuronal Modeling: From Synapses to Networks*. Cambridge, MA: The MIT Press, 291–334.